Nuclear Medicine and Biology 40 (2013) 933–938

Contents lists available at ScienceDirect

Nuclear Medicine and Biology

journal homepage: www.elsevier.com/locate/nucmedbio

Application of ^{99m}Technetium-HYNIC(tricine/TPPTS)-Aca-Bombesin(7-14) SPECT/CT in prostate cancer patients☆,☆☆ A first-in-man study

Hildo J.K. Ananias [a,*], Zilin Yu [b], Hilde D. Hoving [a], Stefano Rosati [c], Rudi A. Dierckx [b], Fan Wang [d], Yongjun Yan [e], Xiaoyuan Chen [e], Jan Pruim [b,h], Marjolijn N. Lub-de Hooge [b,f], Wijnand Helfrich [g], Philip H. Elsinga [b], Igle J. de Jong [a]

[a] Department of Urology, University Medical Center Groningen, University of Groningen, Groningen, The Netherlands
[b] Department of Nuclear Medicine and Molecular Imaging, University Medical Center Groningen, University of Groningen, Groningen, The Netherlands
[c] Department of Pathology, University Medical Center Groningen, University of Groningen, Groningen, The Netherlands
[d] Medical Isotopes Research Center, Peking University, Peking, China
[e] Laboratory of Molecular Imaging and Nanomedicine, National Institute of Biomedical Imaging and Bioengineering, National Institutes of Health, Bethesda, MD, USA
[f] Hospital and Clinical Pharmacy, University Medical Center Groningen, Groningen, The Netherlands
[g] Department of Surgery, Laboratory of Translational Surgical Oncology, University Medical Center Groningen, University of Groningen, Groningen, The Netherlands
[h] Department of Nuclear Medicine, Tygerberg Hospital, Stellenbosch University, Stellenbosch, South-Africa

ARTICLE INFO

Article history:
Received 4 November 2012
Received in revised form 20 May 2013
Accepted 27 May 2013

Keywords:
Prostate cancer
SPECT/CT
Bombesin
GRPR
First-in-man

ABSTRACT

Rationale: The peptide bombesin (BBN) and its derivatives exhibit high binding affinity for the gastrin-releasing peptide receptor (GRPR), which is highly expressed in prostate cancer. We used the BBN-based radiopharmaceutical ^{99m}Technetium-HYNIC(tricine/TPPTS)-Aca-Bombesin(7-14) (^{99m}Tc-HABBN) to perform a first-in-man clinical pilot study to evaluate the feasibility of ^{99m}Tc-HABBN SPECT/CT for detection of prostate cancer in patients.

Methods: Eight patients with biopsy-proven prostate cancer who were scheduled for either radical prostatectomy or external beam radiotherapy underwent ^{99m}Tc-HABBN scintigraphy and SPECT/CT prior to treatment. Serial blood samples were taken to assess blood radioactivity and to determine *in vivo* metabolic stability. Clinical parameters were measured and reported side effects, if present, were recorded. Prostate cancer specimens of all patients were immunohistochemically stained for GRPR.

Results: ^{99m}Tc-HABBN was synthesized with high radiochemical yield, purity and specific activity. There were no significant changes in clinical parameters, and there were no adverse or subjective side effects. Low metabolic stability was observed, as less than 20% of ^{99m}Tc-HABBN was intact after 30 min. Immunohistochemical staining for GRPR was observed in the prostate cancer specimens in all patients. ^{99m}Tc-HABBN scintigraphy and SPECT/CT did not detect prostate cancer in patients with proven disease.

Conclusions: ^{99m}Tc-HABBN SPECT/CT for visualization of prostate cancer is safe but hampered by an unexpected low *in vivo* metabolic stability in man. The difference between the excellent *in vitro* stability of ^{99m}Tc-HABBN in human serum samples determined in our previous study regarding ^{99m}Tc-HABBN and the low *in vivo* metabolic stability determined in this study, is striking. This issue warrants further study of peptide-based radiopharmaceuticals.

1. Introduction

Prostate cancer is one of the most common causes of cancer in males and is a common cause of morbidity and death worldwide [1]. Early detection of prostate cancer may lead to an improved cure rate. An increased level of prostate-specific antigen (PSA) in serum or a palpable prostatic nodule found with digital rectal examination raises the suspicion of prostate cancer and necessitates transrectal ultrasound-guided biopsies of the prostate for histological diagnosis.

☆ Conflict of Interest statement: All authors have no financial relationship with the organization that sponsored the research and have no conflict of interest.

☆☆ Financial support: This work was supported by grants from the Dutch Cancer Society (KWF 2008-4243), the Dutch Urology Foundation 1973 (Stichting Urologie 1973), the Jan Kornelis de Cock Stichting (J.K. de Cock Stichting 08-02) and the Center for Translational Molecular Medicine (project Prostate Cancer Molecular Medicine 03O-203).

* Corresponding author. Department of Urology, University Medical Center Groningen, Hanzeplein 1, 9712 RB, Groningen, the Netherlands. Tel.: +31 503619952; fax: +31 503619607.
E-mail address: h.j.k.ananias@umcg.nl (H.J.K. Ananias).

0969-8051/$ – see front matter © 2013 Elsevier Inc. All rights reserved.
http://dx.doi.org/10.1016/j.nucmedbio.2013.05.009

Although performing transrectal ultrasound-guided biopsies is the gold standard procedure, it has certain drawbacks, such as the chance of under- or overstaging due to sampling error in multifocal disease [2]. Furthermore, transrectal ultrasound-guided biopsies have a suboptimal sensitivity, as they can miss up to 35% of cancers [3–5]. A negative (repeat) biopsy, despite a persistently elevated PSA, poses a diagnostic dilemma [6,7].

An imaging technique that is sufficiently sensitive to detect prostate cancer and/or sufficiently specific to exclude cancer is necessary. In addition to detection and local staging of prostate cancer, other possible uses of such an imaging technique could be the guidance for prostate biopsies, application of intensity-modulated radiotherapy on hot-spots, detection of distant metastases or local recurrence and therapy response monitoring.

Nuclear imaging techniques such as single photon emission computed tomography (SPECT) and positron emission tomography (PET) have emerged as promising diagnostic tools in oncology [8–10]. Of the available radiopharmaceuticals for prostate cancer detection, ^{18}F PET/CT and ^{11}C-choline PET/CT are mostly used in centers all worldwide, as they are currently the best-performing nuclear imaging techniques. However, the limited sensitivity for small-sized metastases, relatively low uptake of choline at low PSA levels and uptake of choline in normal or inflamed prostate limit the accuracy of choline PET/CT in staging prostate cancer [10,11]. Therefore, crucial for accurate new nuclear imaging techniques is the development of radiopharmaceuticals that can be targeted to specific tumor-associated antigens, which are over-expressed in prostate cancer but are sparse in normal tissues.

A tumor-associated antigen that is of particular interest is the gastrin-releasing peptide receptor (GRPR). GRPR is over-expressed in various human malignancies, including primary and metastatic prostate cancer [12,13]. Importantly, GRPR expression in normal tissue ranges from absent to low [14–17], making GRPR an excellent target for high-contrast imaging. The mammalian ligand for GRPR and its amphibian counterpart bombesin (BBN) share an identical seven-amino-acid carboxyl-terminal region, and both possess the same affinity for GRPR. However, BBN has been shown to be significantly more stable, and a series of BBN analogs has been constructed and labeled with various radionuclides (i.e., ^{99m}Tc, ^{111}In, ^{64}Cu, ^{18}F) [18,19].

Recently, we reported the synthesis of ^{99m}Tc-HYNIC(tricine/TPPTS)-Aca-BBN(7–14) (from here on: ^{99m}Tc-HABBN; HYNIC = 6-hydrazinonicotinic acid; TPPTS = trisodium triphenylphosphine-3,3′,3″-trisulfonate; Aca = ε-Amino-caproic acid) and its promising results as an imaging agent in a xenograft tumor model for human prostate cancer in athymic mice [20].

The aim of the study described in this report was to perform a first-in-man clinical pilot study to evaluate the feasibility of ^{99m}Tc-HABBN SPECT/CT for detection of prostate cancer in patients.

2. Material and methods

2.1. Chemicals, materials and equipment

Na^{99m}TcO$_4$ was eluted from the ^{99}Mo/^{99m}Tc generator (Ultra-Technekow; Covidien, Petten, The Netherlands). Succinic acid and tricine (N-(Tri(hydroxymethyl)methyl)glycine) were purchased from Sigma/Aldrich (St. Louis, MO, USA). TPPTS was purchased from Alfa Aesar (Karlsruhe, Germany). The peptide Aca-BBN(7–14) was provided by Peptides International (Louisville, KY, USA). HYNIC-Aca-BBN(7–14) was synthesized as reported previously [20]. For sterilization, a 0.22-μm Millex GV-filter (Merck Millipore, Billerica, MA, USA) was used. High-performance liquid chromatography (HPLC) was performed using a HITACHI L-2130 HPLC system (Hitachi High Technologies America Inc., Pleasanton, CA, USA). Isolation of radiolabeled peptides was performed using a Phenomenex reversed-phase Luna C18 column (Phenomenex, Torrance, CA, USA). The Sep-Pak C18 light cartridge was from Waters Corporation (Milford, MA, USA). Radioactivity of samples was measured in a γ-counter (Compugamma CS1282; LKB-Wallac, Turku, Finland).

For immunohistochemistry experiments, PC-3 human prostate cancer xenograft tumors (ATCC, Manassas, VA, USA), normal goat serum, 0.05% 3,3′-diaminobenzidine, Eukitt mounting medium, 1% AB serum (Sigma-Aldrich, St. Louis, MO, USA), hematoxylin (Merck, Whitehouse Station, NJ, USA), anti-human-GRPR rabbit polyclonal antibody ab39963 (Abcam, Cambridge, UK) and goat anti-rabbit antibody P0448 (Dako, Glostrup, Denmark) were used.

2.2. Preparation of ^{99m}Tc-HABBN

Synthesis of ^{99m}Tc-HABBN was performed as described previously [20] under GMP conditions with modifications. All solutions (except the HYNIC-Aca-BBN(7–14) and the $SnCl_2$ solution) were sterilized before use by passing through a 0.22-μm Millex GV-filter under aseptic conditions (class A) in a cleanroom. Briefly, ^{99m}Tc-pertechnetate solution (~2.8 GBq in saline, ~2 mL) was collected in a sterile vial (5 mL). 50 μL of HYNIC-Aca-BBN(7–14) (1 mg/mL in sterile water), 100 μL of tricine solution (100 mg/mL in 25 mM succinate buffer, pH 5.0), 100 μL of TPPTS solution (50 mg/mL in 25 mM succinate buffer, pH 5.0) and 15 μL of $SnCl_2$ (1.0 mg/mL in water) were added to the vial and well mixed. The pH value (pH 5.0) of the mixture was checked with pH paper, and then the mixture was incubated at 95 °C for 20 min. A needle connected to a 0.22-μm Millex GV-filter was placed in the cap of the vial to avoid overpressure and contamination.

After cooling to room temperature, the reaction mixture was purified with semi-preparative reversed-phase HPLC column equipped with a UV detector (wave length = 218 nm) and a radioactivity detector. Isolation of ^{99m}Tc-HABBN was performed using a Phenomenex reversed-phase Luna C18 column (10 mm × 250 mm, 5 μm) with a flow rate at 2.5 mL/min. A gradient system was applied for isolation of ^{99m}Tc-HABBN, starting from 90% solvent A (0.01 M phosphate buffer with 0.1 mg/mL ascorbic acid (AA), pH = 6.0) and 10% solvent B (acetonitrile (ACN) with 0.1 mg/mL AA) (5 min) and ramped to 45% solvent A and 55% solvent B at 35 min.

The ^{99m}Tc-HABBN eluate from the HPLC system was diluted with saline with 1% AA (10 mL) before loading on a Sep-PAK C18 light cartridge. The C18 cartridge was washed with saline with 1% AA (50 mL) and eluted with EtOH (400 μL) afterwards. The EtOH solution was diluted with saline solution (with 1% AA; limit: ~10 mL) and was sterilized by passing through a 0.22-μm GV-filter. A quantity of 550–700 MBq was dispensed in a syringe under aseptic conditions (class A).

2.3. Quality control of ^{99m}Tc-HABBN

Before release of the final product, the integrity of the 0.22-μm Millex GV filter (used for sterilization of the final product) was determined using the bubble point test, and the radiochemical purity of the final product was determined by analyzing a 5-MBq portion using HPLC. After release, the sterility test was performed by keeping two samples (100 μL) of the final product in two bottles of Clausen medium at 25 °C and 37 °C for 1 week. The remaining product was used for the pyrogenicity test, the residual solvents test and the EtOH concentration test performed at the Pharmacy Department of the University Medical Center Groningen after decay.

2.4. Patient recruitment

The present study was approved by the Medical Ethics Committee of the University Medical Center Groningen and was performed according to Good Clinical Practice guidelines.

Eight patients with biopsy-proven prostate cancer (four patients scheduled for laparoscopic radical prostatectomy (RP), and four planned for external beam radiotherapy (EBRT)) were recruited on the outpatient clinic of the department of Urology at the University Medical Center Groningen, after providing written informed consent. The pre-therapy PSA level, prostate volume as determined by transrectal ultrasound, tumor stage (according to the 1997 TNM staging criteria), results of prostate histology (either *via* whole prostatectomy specimens or prostate biopsies; Gleason sum score, % tumor volume) and results of pelvic lymph node dissection (1/4 in the RP group, 4/4 in the EBRT group) were recorded.

2.5. Scintigraphy, SPECT/CT and image analysis

SPECT/CT scanning was performed before EBRT or 1 day before surgery. Subjects were positioned supine with their arms outstretched in holders, and a venous cannula was placed in both forearms—left for injection of the radiopharmaceutical and right for blood sampling. For low-dose computed tomography, the arms were positioned above the head. Images of the pelvis were performed using a Siemens Symbia T2 double headed gamma camera, equipped with low-energy, high-resolution collimators, combined with an integrated 2-slice computed tomography. To acquire quantitative results, a sample of ^{99m}Tc of known activity (20–28 MBq) was scanned along with the patient.

Different data acquisition protocols were used to acquire an optimal time-point for scanning. Patients 1–4 were subjected to a dynamic scanning protocol with the gamma camera heads in the anterior–posterior (AP) position, 1 min per frame during 20 min, starting immediately after ^{99m}Tc-HABBN injection (549–688 MBq). Thereafter, a 2 × 180° SPECT of the pelvic region was performed with a matrix size of 128 × 128 in 64 positions and an acquisition time of 40 s per position. Next, a low-dose CT of the pelvis was performed (110 kV, 30 mA). At 2, 4, 6 and 20 h post-injection (p.i.), SPECT was performed again at the 20 h-time-point combined with low-dose CT. Patient 5 was subjected to a dynamic scan for 120 min with the gamma camera in the AP position at 1 min per frame during the first hour and 2 min per frame during the second hour. At 4, 6 and 20 h p.i., a static scan in the AP position was made for 10, 30 and 30 min, respectively. In patients 6–8, a dynamic scan was made for 60 min, 1 min per frame, followed by SPECT/CT and single-frame, 30-min static images at 2, 4 and 6 h p.i. Additionally, in patients 3, 4, 6, 7 and 8, a transurethral catheter was inserted to drain the bladder and reduce local radioactivity.

Images were reconstructed using iterative reconstruction (Flash 3D, 8 iterations, 16 subsets, Gaussian 9.0 filter). In addition to anatomical localization, CT was also used to obtain an attenuation map. Dynamic and static images were displayed in coronal planes, and SPECT images were displayed in transaxial, coronal and sagittal planes. The tumor to normal tissue ratios were determined by placing a region of interest (ROI) over the area showing the most activity in the tumor and an identically sized ROI over the gluteal muscles. Image analysis and subjective assessment were performed by a nuclear physician (JP) blinded to patient data and 1 non-blinded researcher (HA).

2.6. Monitoring of vital parameters and side effects

Because this was a first-in-man study, the heart rate, oxygen saturation and blood pressure were monitored in all patients during the first hour p.i. at regular intervals (0, 5, 10, 15, 20, 25, 30, 45 and 60 min) and were compared with baseline measurements before injection of ^{99m}Tc-HABBN. Side effects, if reported by the patient within 24 h p.i., were documented.

2.7. Analysis of radioactivity in blood samples

Blood samples (2 mL/time point) were collected from six patients *via* a venous cannula in the right forearm at 0, 2, 5, 10, 30, 60, 120, 240, 360 and 1200 min (the last time point was not analyzed for patients 7 and 8) p.i. of ^{99m}Tc-HABBN. No blood sampling of patients 2 and 6 was performed due to technical failure.

Blood serum samples were acquired by centrifuging the blood sample at 3000 rpm for 5 min. For each sample, the radioactivity of full blood and blood serum (250 μL), as well as the original ^{99m}Tc-HABBN saline solution (10 μL in triplicate) was determined in a γ-counter. The radioactivity accumulation of ^{99m}Tc-HABBN in full blood and serum was calculated as follows: counts of the 250-μL sample *4 / total injected counts (percentage of the injected dose/mL, mean ± SD, n = 6).

2.8. Metabolic stability of ^{99m}Tc-HABBN

The *in vivo* metabolic stability of ^{99m}Tc-HABBN was determined by analyzing blood serum samples collected at 0 (baseline), 2, 5, 10, 30, 60 and 120 min p.i. of ^{99m}Tc-HABBN from patients 1, 3, 4 and 5. Blood serum samples were acquired as described above. The protein of blood serum samples was removed by centrifuging at 3000 rpm for 5 min after mixing with a 10-fold volume of ACN. The supernatant was passed through a Sep-Pak C18 light cartridge and eluted with water (5 mL) and EtOH (2 mL). The radioactivity of the eluents was determined in a γ-counter. The percentage of metabolites was calculated as follows: (aqueous eluent radioactivity / (aqueous eluent radioactivity + EtOH eluent radioactivity)) * 100% (mean ± SD, n = 4).

2.9. Immunohistochemical staining of GRPR

In patients scheduled for RP, prostatectomy specimens were used for immunohistochemical staining of GRPR. In patients who did not undergo RP, prostate biopsy specimens were used.

Formalin-fixed, paraffin-embedded blocks of prostate cancer tissue were cut into 3-μm thick sections and mounted on APES (3-aminopropyltriethoxysilane)-coated slides. A human prostate cancer PC-3 xenograft tumor was used as the positive control. As the negative control, the primary antibody was omitted during immunohistochemical analysis on the positive control tissue. Tris-buffered saline (TBS) was used for washing and dilution of antibodies. After deparaffinization, antigen retrieval was performed by microwave heating (400 W) for 20 min in a 0.1 M Tris/HCl buffer at pH 9.0. Endogenous peroxidase was blocked by incubation with 0.3% hydrogen peroxide in TBS for 20 min. To decrease non-specific background staining, slides were incubated with normal goat serum diluted at 1:10 in TBS for 30 min at room temperature.

Tissue section slides were incubated with primary anti-human-GRPR rabbit polyclonal antibody ab39963 diluted at 1:250 in 1% bovine serum albumin (BSA)/TBS overnight at 4 °C. A secondary step with goat anti-rabbit antibody P0448 diluted at 1:100 in 1% BSA/TBS with 1% AB serum was applied for 60 min at room temperature. Slides were immersed for 10 min in a solution of 0.05% 3,3′-diaminobenzidine and 0.03% hydrogen peroxide in TBS for visualization of the signal as brown staining. After washing with demineralized water, slides were counterstained with hematoxylin and dehydrated. Finally, a coverslip was applied using Eukitt mounting medium.

2.10. Assessment of GRPR staining

An experienced pathologist (SR) blinded to the clinical data scored the staining intensity (0 = no staining, 1+ = weak staining, 2+ = moderate staining, 3+ = strong staining) of tumor areas for all specimens. Specimens, in which one or more tumor areas with different staining intensities were present, were scored for the most prevalent intensity.

Table 1
Release and post-release specifications for ^{99m}Tc-HABBN.

^{99m}Tc-HABBN	Specification	Required before release	Frequency
Appearance	Clear, colorless	Yes	Every synthesis
pH	5–8	Yes	Every synthesis
Radiochemical purity (%)	>95%	Yes	Every synthesis
Specific activity (MBq/mg)	>5000	Yes	Every synthesis
Bubble point test sterilization filter	<20%	Yes	Every synthesis
Sterility	Sterile	No	Every synthesis
Endotoxins (EU/mL)	<0.25	No	Every synthesis
EtOH concentration (g/L)	<100	No	Every synthesis
ACN concentration (mg/L)	<50	No	Every synthesis

3. Results

3.1. Synthesis and quality control of ^{99m}Tc-HABBN

^{99m}Tc-HABBN was prepared (n = 8) with a radiochemical yield of 43% ± 4%, a specific activity of 87.2 ± 9.4 TBq/mmol and a radiochemical purity of 97.3% ± 0.9%. The bubble point test of the sterilization filter was performed before the injection of ^{99m}Tc-HABBN. The sterility, endotoxin and residual solvents tests were performed after release of the radiotracer. The final product was sterile and apyrogenic (<0.25 EU/mL), and residual solvents were found to be <50 mg/L and <100 g/L for ACN and EtOH, respectively. Release and post-release specifications are summarized in Table 1.

3.2. Patient characteristics

Details of included patients and results of histology can be found in Table 2. Although initially selected for EBRT, patients 7 and 8 proved to have lymph node metastases and were subsequently selected for hormonal therapy.

3.3. Image analysis

Thorough analysis of the dynamic, static and SPECT images with or without CT by one dedicated nuclear medicine physician (JP) blinded to patient data and one non-blinded researcher (HA), revealed no uptake of radioactivity in the prostate or pelvic lymph nodes (histologically proven lymph node metastases in patients 7 and 8). Rapid distribution *via* blood was observed, and excretion *via* urine was observed within 5–7 min. The transurethral catheter reduced radioactivity in the pelvis, improving visualization of tissue in the immediate vicinity of the bladder. The procedure did not lead to detection of a hot-spot in the prostate. Furthermore, no hot-spots outside the bladder or prostate were observed in the pelvis. No ROIs were drawn because the tumor was not visualized.

3.4. Monitoring of vital parameters and side effects

In the first hour after ^{99m}Tc-HABBN injection, vital parameters (heart rate, oxygen saturation and blood pressure) were measured at regular intervals and were compared with baseline measurements. No clinically significant changes in the heart rate (>15% change), oxygen saturation (>5% change) and blood pressure (>15% change) were recorded. None of the patients suffered from adverse or subjective side effects.

3.5. Analysis of radioactivity in blood

Fig. 1 shows the full blood and serum radioactivity curves after ^{99m}Tc-HABBN injections in patients during the 1200-min study period (n = 6, except at the 1200-min time point where n = 4). A steady decline of the radioactivity was observed in blood and serum during the experimental period. The radioactivity level became almost undetectable at 20 h p.i.

3.6. Metabolic stability of ^{99m}Tc-HABBN

Fig. 2 shows the *in vivo* degradation of ^{99m}Tc-HABBN. There are low metabolic stability and rapid degradation of ^{99m}Tc-HABBN, with 22%, 44% and 53% of the radioactivity degraded within 2, 5 and 10 min p.i., respectively. After 30 min, less than 20% of ^{99m}Tc-HABBN was still intact.

3.7. Assessment of immunohistochemical GRPR staining

Immunohistochemistry on paraffin slides of prostate cancer specimens (four whole prostate sections, four prostate needle biopsy specimens) demonstrated low-to-moderate staining of prostate cancer for GRPR in 8/8 cases (Table 3).

4. Discussion

Targeted imaging could improve the lack of accuracy observed in current imaging techniques used in different stages of prostate cancer. Recently, we have developed the novel BBN-based radiopharmaceutical, designated ^{99m}Tc-HABBN, and evaluated its imaging potential in a xenograft mouse model of human prostate cancer [20]. The aim of the study presented here was to perform a first-in-man clinical pilot study to evaluate the feasibility of ^{99m}Tc-HABBN SPECT/CT for detection of prostate cancer in patients. We were able to synthesize a radiopharmaceutical with high yield, specific activity and purity, in the absence of any signs of adverse or subjective side effects after patient

Table 2
Patient characteristics.

Pt. nr.	Age	PSA	PrV	Therapy	T-stage	TumorV	Gl	PLND
1	59	5,9	35	RP	pT2c[a]	5%[a]	7[a]	np
2	55	16	21	RP	pT2c[a]	>50%[a]	6[a]	np
3	69	12	47	RP	pT2c[a]	<50%[a]	7[a]	pN0
4	73	7,8	56	EBRT	cT1c[b]	Left/5/5/75%, Right/5/1/5%[c]	7[c]	pN0
5	55	15,5	23	RP	pT3a[a]	>50%, capsular penetration left[a]	8[a]	np
6	73	69.8	38	EBRT	cT2c[b]	Left/5/2/15%, Right/5/4/45%[c]	9[c]	pN0
7	71	221.5	55	HT	cT3[b]	Left/4/4/65%, Right/4/4/10%[c]	7[c]	pN1
8	70	23.8	39	HT	cT2c[b]	Left/4/4/35%, Right/4/4/20%[c]	7[c]	pN1

Biopsy results are not displayed when histology of a radical prostatectomy is available. In EBRT or hormonal therapy patients, only prostate biopsy histology is available. Age in years, PSA in ng/mL, PrV = prostate volume in mL, RP = radical prostatectomy, EBRT = external beam radiotherapy, HT = hormonal therapy, T-stage = tumor stage.
TumorV = % tumor volume (tumor volume based on prostate biopsies are presented as follows: side/biopsy cores taken on that side/number of positive cores on that side/%tumor volume), Gl = Gleason sum score, PLND = pelvic lymph node dissection, np = not performed, pN0 = no pelvic lymph node metastases, pN1 = pelvic lymph node metastases.
[a] Based on histology of radical prostatectomy specimens, [b] Based on digital rectal examination and histology of prostate biopsies, [c] Based on histology of prostate biopsies.

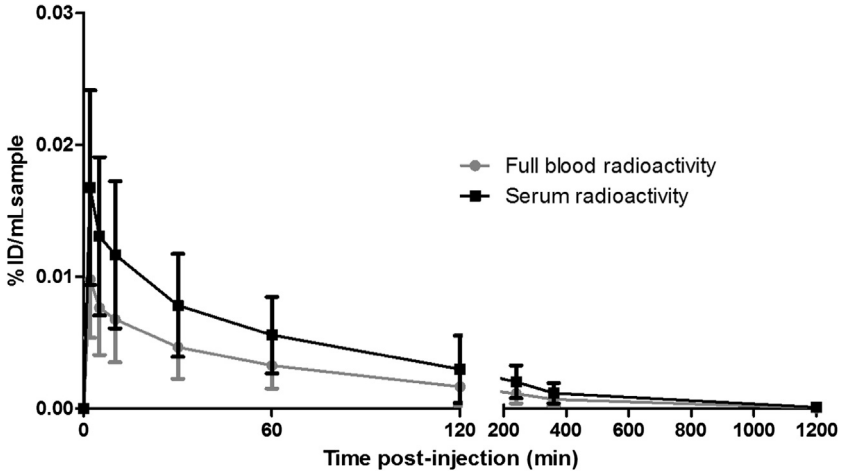

Fig. 1. Full blood and serum activity curves during the 1200-min study. Values are expressed as the percentage of the injected dose per mL (%ID/mL, mean ± SD, n = 6, except at the 1200-min time point where n = 4).

administration. However, ^{99m}Tc-HABBN scintigraphy and SPECT/CT did not detect prostate cancer in patients with proven disease.

Although immediate distribution *via* the vascular system and rapid excretion *via* the renal route were deduced from the dynamic images, no uptake in the prostate was observed at any time point in any patient. Although bladder drainage using a transurethral catheter proved to be helpful in reducing activity in the bladder with an improved ability to assess pelvic organs, it did not aid in detecting hot-spots.

Because small tumors could be missed with SPECT, patients with larger tumor volumes and higher PSA values were selected in the second half of the patient inclusion (patients 5–8). The different patient selection sorted no effect. Additionally, there has been some discussion concerning the level of GRPR expression according to various Gleason sum scores. Although this could not be proven in lymph node and bone metastases of prostate cancer [12], Beer et al. demonstrated that a higher Gleason sum score tends to express lower levels of GRPR [13]. Therefore, a range of Gleason sum scores was selected (Gleason 6–9; lower scores are seldom observed, and Gleason 10 is only rarely eligible for local therapy), but did not give other results with ^{99m}Tc-HABBN scintigraphy and SPECT/CT. One reason for the failure to visualize the prostate tumors is that, by chance, GRPR expression in 8 prostate cancer patients could be absent. However, with immunohistochemistry on paraffin slides of the prostate cancer specimens of these patients, we proved the presence of GRPR in all our patients (Table 3). Although immunohistochemistry shows the presence and tissue distribution of an antigen, the technique cannot demonstrate absolute antigen density and is therefore not a strong predictor for uptake of a GRPR-targeting radiopharmaceutical.

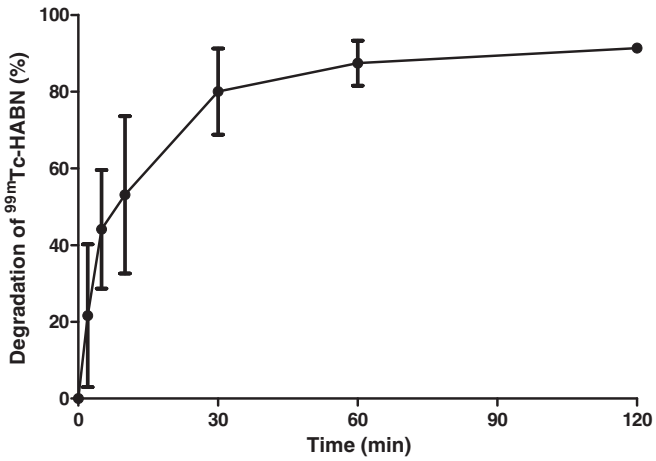

Fig. 2. The *in vivo* metabolic stability of ^{99m}Tc-HABBN. Results are plotted as the percentage of formed metabolites at different time points (mean ± SD, n = 4). At the 120-min time point, the SD is too small to display.

The difference between the *in vitro* stability in human serum samples determined in our previous study on ^{99m}Tc-HABBN [20] and the *in vivo* metabolic stability determined in the present study, is striking. In our previous study, we have demonstrated that 77% of ^{99m}Tc-HABBN is intact after 24 h in human serum *in vitro* [20]. However, the results of the current study indicate that metabolites are formed as early as 10 min p.i. and that less than 20% of ^{99m}Tc-HABBN is intact after 30 min. Thus, we must conclude that one of the main reasons for the failure to visualize the prostate tumors is the rapid *in vivo* degradation of ^{99m}Tc-HABBN (Fig. 2). Similar results were observed in a study by Linder et al., where the metabolism of ^{177}Lu-AMBA in mice and rats *in vivo* was much more rapid than that *in vitro* [21].

Rapid and highly selective proteolytic cleavage of bioactive peptides is not unexpected because this is key in the autonomic regulation of the biologic effects of peptides. It is unknown which enzymes are responsible for the degradation of BBN *in vivo*. In this respect, ecto-enzymes located on the cell surface that shed in blood and are highly expressed in the liver and kidneys could be major players in this process [22]. Therefore, to more accurately determine radiochemical stability, it was suggested by Ocak et al. to use liver and kidney homogenates [23]. By contrast, in another study by the same author, it was shown that rat liver and kidney homogenates were not good predictors for *in vivo* stability [24].

In a pre-clinical study in a xenograft tumor model for human prostate cancer in athymic mice, we have demonstrated moderate uptake of ^{99m}Tc-HABBN in tumors [20]. Moderate uptake in tumors

Table 3
Staining intensities of the antibodies used in prostate cancer specimens.

Patient number	Pathology	Staining intensity
1	Radical prostatectomy	+
2	Radical prostatectomy	+
3	Radical prostatectomy	+
4	Prostate needle biopsy	+
5	Radical prostatectomy	+
6	Prostate needle biopsy	+
7	Prostate needle biopsy	++
8	Prostate needle biopsy	+

does not pose a real problem provided that the background uptake is low to create high tumor-to-background ratios and excellent contrast. Performance of a BBN-like radiopharmaceutical in a pre-clinical mouse model is not a strong predictor for clinical performance in humans because there is a different body biodistribution of GRPR in mice compared with humans. Nevertheless, the moderate uptake of ^{99m}Tc-HABBN in tumor cells as previously demonstrated in the pre-clinical study could be another contributing factor leading to failure to visualize the prostate tumors in prostate cancer patients in this study.

Other clinical studies in prostate cancer patients with BBN-like radiopharmaceuticals have shown fairly good results [19]. A study by Scopinaro et al. is particularly interesting because high uptake in the prostate was found in all eight prostate cancer patients, and pathology-confirmed invasion in obturator nodes was found in three of these patients [26]. Despite the clinical results of other groups and the findings of our pre-clinical study where the prostate tumor was clearly visualized in mice with ^{99m}Tc-HABBN microSPECT, we could not detect prostate cancer with ^{99m}Tc-HABBN scintigraphy and SPECT/CT in patients of the current clinical study. Two main reasons for the inability to detect prostate cancer with scintigraphy and SPECT/CT are most likely the low *in vivo* stability of ^{99m}Tc-HABBN resulting in low-circulating intact radiopeptide and the absolute tumor uptake of ^{99m}Tc-HABBN being too low because of the relatively low to moderate expression of GRPR in primary prostate cancer. When considering the IC_{50}, the *in vivo* tumor uptake and tumor-to-normal-tissue ratios in the pre-clinical study, the affinity and performance of ^{99m}Tc-HABBN are essentially similar compared with other BBN analogs reported in the literature [19,25]. The pre-clinical data of the BBN-like radiopharmaceuticals that have been used for imaging of prostate cancer patients are not available in the international literature and, therefore, cannot be compared with our pre-clinical data.

The findings that the *in vitro* stability of a BBN-like radiopharmaceutical in human serum does not correlate with *in vivo* stability and that the *in vivo* performance of a BBN-like radiopharmaceutical in a mouse tumor model does not correlate with *in vivo* performance in man are interesting. As demonstrated previously, determination of the stability of a radiolabeled peptide *in vitro* in serum has no predictive value for its *in* vivo stability in rodents [21,23,24]. The development of new or improved *in vitro* stability tests or better pre-clinical *in vivo* tumor models may prove to be a better approach for selecting radiolabeled peptides of appropriate stability and affinity for clinical testing. Future studies should focus on developing high-affinity BBN-like radiopharmaceuticals that have been proven to be highly stable in a pre-clinical setting. Additionally, instead of using the relatively low-resolution SPECT for imaging, the use of radiopeptides suitable for PET imaging will aid in improvement of imaging.

5. Conclusions

^{99m}Technetium-HYNIC(tricine/TPPTS)-Aca-Bombesin(7–14) SPECT/CT for the detection of prostate cancer is safe but is hampered by an unexpectedly low *in vivo* metabolic stability in man. The difference between the excellent *in vitro* stability in human serum determined in our previous study on ^{99m}Tc-HABBN and the low *in vivo* metabolic stability determined in the present study is striking. Furthermore, the current study showed that the *in vivo* performance in a mouse tumor model does not correlate with *in vivo* performance in prostate cancer patients. This issue warrants further study of peptide-based radiopharmaceuticals.

Acknowledgments

We thank Karin Groeneveld, Remko Koning, Jose Douma, Hans ter Veen, Johan Wiegers and Johan de Jong for assistance with SPECT/CT imaging and protocol development. This work was supported by grants from the Dutch Cancer Society (KWF 2008-4243), the Dutch Urology Foundation 1973 (Stichting Urologie 1973), the Jan Kornelis de Cock Stichting (J.K. de Cock Stichting 08-02) and the Center for Translational Molecular Medicine (project Prostate Cancer Molecular Medicine 03O-203).

References

[1] Center MM, Jemal A, Lortet-Tieulent J, Ward E, Ferlay J, Brawley O, et al. International variation in prostate cancer incidence and mortality rates. Eur Urol 2012;61(6):1079–92.
[2] Arora R, Koch MO, Eble JN, Ulbright TM, Li L, Cheng L. Heterogeneity of Gleason grade in multifocal adenocarcinoma of the prostate. Cancer 2004;100(11):2362–6.
[3] Eichler K, Hempel S, Wilby J, Myers L, Bachmann LM, Kleijnen J. Diagnostic value of systematic biopsy methods in the investigation of prostate cancer: a systematic review. J Urol 2006;175(5):1605–12.
[4] Chang JJ, Shinohara K, Bhargava V, Presti Jr JC. Prospective evaluation of lateral biopsies of the peripheral zone for prostate cancer detection. J Urol 1998;160(6 Pt 1):2111–4.
[5] Presti Jr JC, Chang JJ, Bhargava V, Shinohara K. The optimal systematic prostate biopsy scheme should include 8 rather than 6 biopsies: results of a prospective clinical trial.J Urol 2000;163(1):163–6 [discussion 166–7].
[6] Levy DA, Jones JS. Management of rising prostate-specific antigen after a negative biopsy. Curr Urol Rep 2011.
[7] Resnick MJ, Lee DJ, Magerfleisch L, Vanarsdalen KN, Tomaszewski JE, Wein AJ, et al. Repeat prostate biopsy and the incremental risk of clinically insignificant prostate cancer. Urology 2011;77(3):548–52.
[8] Mariani G, Bruselli L, Kuwert T, Kim EE, Flotats A, Israel O, et al. A review on the clinical uses of SPECT/CT. Eur J Nucl Med Mol Imaging 2010;37(10):1959–85.
[9] Ambrosini V, Fani M, Fanti S, Forrer F, Maecke HR. Radiopeptide imaging and therapy in Europe. J Nucl Med 2011;52(Suppl. 2):42S–55S.
[10] De Jong IJ, De Haan TD, Wiegman EM, Van Den Bergh AC, Pruim J, Breeuwsma AJ. PET/CT and radiotherapy in prostate cancer. Q J Nucl Med Mol Imaging 2010;54(5):543–52.
[11] Jadvar H. Prostate cancer: PET with 18F-FDG, 18F- or 11C-acetate, and 18F- or 11C-choline. J Nucl Med 2011;52(1):81–9.
[12] Ananias HJ, van den Heuvel MC, Helfrich W, de Jong IJ. Expression of the gastrin-releasing peptide receptor, the prostate stem cell antigen and the prostate-specific membrane antigen in lymph node and bone metastases of prostate cancer. Prostate 2009;69(10):1101–8.
[13] Beer M, Montani M, Gerhardt J, Wild PJ, Hany TF, Hermanns T, et al. Profiling gastrin-releasing peptide receptor in prostate tissues: clinical implications and molecular correlates. Prostate 2012;72(3):318–25.
[14] Aprikian AG, Cordon-Cardo C, Fair WR, Reuter VE. Characterization of neuroendocrine differentiation in human benign prostate and prostatic adenocarcinoma. Cancer 1993;71(12):3952–65.
[15] Cutz E, Chan W, Track NS. Bombesin, calcitonin and leu-enkephalin immunoreactivity in endocrine cells of human lung. Experientia 1981;37(7):765–7.
[16] Price J, Penman E, Wass JA, Rees LH. Bombesin-like immunoreactivity in human gastrointestinal tract. Regul Pept 1984;9(1–2):1–10.
[17] Spindel ER, Chin WW, Price J, Rees LH, Besser GM, Habener JF. Cloning and characterization of cDNAs encoding human gastrin-releasing peptide. Proc Natl Acad Sci U S A 1984;81(18):5699–703.
[18] Schroeder RP, van Weerden WM, Bangma C, Krenning EP, de Jong M. Peptide receptor imaging of prostate cancer with radiolabelled bombesin analogues. Methods 2009;48(2):200–4.
[19] Ananias HJ, de Jong IJ, Dierckx RA, van de Wiele C, Helfrich W, Elsinga PH. Nuclear imaging of prostate cancer with gastrin-releasing-peptide-receptor targeted radiopharmaceuticals. Curr Pharm Des 2008;14(28):3033–47.
[20] Ananias HJ, Yu Z, Dierckx RA, van der Wiele C, Helfrich W, Wang F, et al. (99m) technetium-HYNIC(tricine/TPPTS)-Aca-bombesin(7-14) as a targeted imaging agent with microSPECT in a PC-3 prostate cancer xenograft model. Mol Pharm 2011;8(4):1165–73.
[21] Linder KE, Metcalfe E, Arunachalam T, Chen J, Eaton SM, Feng W, et al. In vitro and in vivo metabolism of Lu-AMBA, a GRP-receptor binding compound, and the synthesis and characterization of its metabolites. Bioconjug Chem 2009;20(6):1171–8.
[22] Konkoy CS, Davis TP. Ectoenzymes as sites of peptide regulation. Trends Pharmacol Sci 1996;17(8):288–94.
[23] Ocak M, Helbok A, von Guggenberg E, Ozsoy Y, Kabasakal L, Kremser L, et al. Influence of biological assay conditions on stability assessment of radiometal-labelled peptides exemplified using a 177Lu-DOTA-minigastrin derivative. Nucl Med Biol 2011;38(2):171–9.
[24] Ocak M, Helbok A, Rangger C, Peitl PK, Nock BA, Morelli G, et al. Comparison of biological stability and metabolism of CCK2 receptor targeting peptides, a collaborative project under COST BM0607. Eur J Nucl Med Mol Imaging 2011;38(8):1426–35.
[25] Schroeder RP, Muller C, Reneman S, Melis ML, Breeman WA, de Blois E, et al. A standardised study to compare prostate cancer targeting efficacy of five radiolabelled bombesin analogues. Eur J Nucl Med Mol Imaging 2010;37(7):1386–96.
[26] Scopinaro F, De Vincentis G, Varvarigou AD, Laurenti C, Iori F, Remediani S, et al. 99mTc-bombesin detects prostate cancer and invasion of pelvic lymph nodes. Eur J Nucl Med Mol Imaging 2003;30(10):1378–82.